

Synthesis, characterization and catalytic properties of mesoporous TiHMA molecular sieves: selective oxidation of cycloalkanes

Parasuraman Selvam^{*}, Susanta K. Mohapatra

Solid State and Catalysis Laboratory, Department of Chemistry, Indian Institute of Technology—Bombay, Powai, Mumbai 400076, India

Received 3 October 2003; received in revised form 7 May 2004; accepted 18 May 2004

Available online 20 July 2004

Abstract

Titanium substituted hexagonal mesoporous aluminophosphate (TiHMA) molecular sieves were synthesized and characterized. Various physicochemical studies, viz., X-ray diffraction, transmission electron microscopy, electron diffraction, environmental scanning electron microscopy, thermal analyses, inductively coupled plasma–atomic emission spectroscopy, diffuse reflectance ultraviolet–visible spectroscopy, Fourier transform Raman spectroscopy, temperature programmed desorption of ammonia and nitrogen absorption–desorption isotherms, confirm the substitution of Ti^{4+} ions in the tetrahedral framework of HMA. The catalytic activity of TiHMA was evaluated for the oxidation reactions of cyclic saturated hydrocarbons such as cyclohexane, cyclooctane and cyclododecane. The catalyst exhibits excellent substrate conversion and product selectivity, and that it was found to be truly as a heterogeneous catalyst as the activity was practically unaffected upon recycling. In particular, the oxidation was highly successful for the bulkier cycloalkane molecules. Furthermore, the activity of TiHMA is also compared with mesoporous TiMCM-41 as well as microporous TiAPO-5 and TS-1 catalysts.

© 2004 Elsevier Inc. All rights reserved.

Keywords: Mesoporous; Molecular sieves; Aluminophosphates; Titanium; Cycloalkanes; Cyclohexane; Cyclooctane; Cyclododecane

1. Introduction

Among the numerous titanium-based homogeneous oxidation catalysts, the Sharpless-type catalyst is the best-known example for the selective asymmetric epoxidation reactions [1]. Catalysts such as titanyl acetyl acetate are also reported to be selective for the oxidation of allylic alcohols as well as for epoxidation reactions [2]. However, one of the major drawbacks of these titanium-based homogeneous complexes is that they are not stable in presence of water. On the other hand, titanium-based heterogeneous catalysts show promise for such reactions with good stability [3,4]. In particular, the discovery of titanium substituted microporous molecular sieve catalysts has enabled remarkable progress in the oxidation reactions [5–12]. However, the application of these catalysts is confined to smaller substrate molecules owing to the pore size limitations.

Nevertheless, the utilization of supramolecular arrays of organic amphiphiles as structure directing agents resulted in the synthesis of mesostructured materials, viz., MCM-41 and MCM-48 [13], which overcome the restriction of pore opening for bulky substrates. Hence, the use of metal substituted mesoporous silicates [14] in the area of heterogeneous catalysis has triggered off considerable interest in the synthesis of their aluminophosphate analogues [15–19]. It is of interest to note that the titanium substituted hexagonal mesoporous aluminophosphates (designated as TiHMA) is a better catalyst as compared to the mesoporous silicate analogue, viz., TiMCM-41, for epoxidation of bulky olefins [16] as well as for the oxidation of phenols [18].

Among the numerous reactions of interest, the liquid-phase oxidation of cyclohexane has attracted much attention owing to the importance of high value products [20]. Traditional processes involving stoichiometric amounts of inorganic oxidants produce huge amounts of environmentally unacceptable wastes [21,22]. Furthermore, the process also leads to several other problems like difficulty in separation, recovery and recycling

^{*} Corresponding author. Tel.: +91-22-2576-7155; fax: +91-22-2572-3480/2576-7152.

E-mail address: selvam@iitb.ac.in (P. Selvam).

of the catalysts after reaction as well as the disposal of liquid and solid wastes, deactivation complications, etc., makes it highly unattractive [22–24] and hence catalytic oxidation in the liquid-phase is increasingly important. In this regard, recently, we have reported a few promising heterogeneous catalysts, viz., FeHMA, (Cr)HMA and (Cr)MCM-41, for the oxidation of cyclohexane [25–27]. In this investigation, we present here a detailed account of the synthesis and characterization of TiHMA molecular sieves. We also report here a systematic study on the oxidation of cyclohexane along with bulkier cycloalkanes, viz., cyclooctane and cyclododecane, over TiHMA catalyst. For a comparison, we have employed mesoporous titanium substituted silicate (TiMCM-41) as well as microporous titanium substituted aluminophosphate (TiAPO-5) and silicate (TS-1) catalysts.

2. Experimental

2.1. Starting materials

Phosphoric acid (85%, Qualigens); aluminium isopropoxide (97%, Merck); tetramethyl ammonium hydroxide (TMAOH, 25 wt.% in water, Aldrich); cetyltrimethylammonium chloride (CTAC, 25 wt.% in water, Aldrich); fumed silica (99.8%, Aldrich); cetyltrimethylammonium bromide (CTAB, 99%, Aldrich); titanium isopropoxide (97%, Aldrich); triethylamine (99.5%, Thomas Baker); pseudoboehmite (70%, Vista); cyclohexane (99.5%, Merck); *tert*-butyl hydroperoxide (TBHP, 70% aqueous solution, Lancaster); cyclooctane (99%, Lancaster); cyclododecane (99%, Lancaster); methyl ethyl ketone (MEK, 99.5%, SD fine); glacial acetic acid (>99%, Fischer).

2.2. Synthesis

TiHMA was prepared as per the following procedure: phosphoric acid was first diluted with water, after which aluminium isopropoxide was added under vigorous stirring. The mixture was kept under constant stirring at 343 K for 1 h to hydrolyze aluminium isopropoxide. Then, titanium isopropoxide was diluted to 20% in isopropanol and was added dropwise to the above mixture followed by TMAOH. The slurry was kept under constant stirring for 2 h and finally the surfactant (CTAC) was added and stirred for another 12 h. The pH of the thin milky gel was maintained at 10. The final gel having a (molar) composition of: Al_2O_3 : P_2O_5 : $x\text{TiO}_2$ ($x = 0.02$ – 0.16): CTAC: 2.5TMAOH : $65\text{H}_2\text{O}$ was transferred into a Teflon-lined autoclave and subjected to hydrothermal treatment at 373 K for 72 h. The product obtained was repeatedly washed with distilled water, filtered and dried at 343 K for 12 h. Varying ‘ x ’ from ‘0.02–0.16’, various $([\text{Al} + \text{P}]/\text{Ti})$ molar ratio,

viz., TiHMA(200), TiHMA(100), TiHMA(50) and TiHMA(25), were prepared. The as-synthesized samples were calcined in a tubular furnace at 823 K for 1 h in a flow of N_2 followed by air for 2 h. For a comparative evaluation of the catalytic activity, mesoporous TiMCM-41 ($\text{Si}/\text{Ti} = 50$) as well as microporous TiAPO-5 ($([\text{Al} + \text{P}]/\text{Ti}) = 50$) and TS-1 ($\text{Si}/\text{Ti} = 33$) materials were also synthesized and characterized as per the details outlined elsewhere [28,29].

2.3. Characterization

All the as-synthesized and calcined samples were systematically characterized using several analytical and spectroscopic techniques. Powder X-ray diffraction (XRD) patterns were recorded on a Rigaku–Miniflex diffractometer using a nickel filtered $\text{CuK}\alpha$ radiation ($\lambda = 1.5418 \text{ \AA}$) with a step size of 0.02° . Transmission electron micrograph (TEM) and electron diffraction (ED) were recorded on a Philips 200 microscope operated at 160 kV. The sample (in powder form) was dispersed in ethanol with sonication (Oscar ultrasonics) and placed a drop of it on a carbon coated copper grid (300 mesh; Sigma-Aldrich). Environmental scanning electron micrographs (E-SEM) were recorded on an ESEM-FEI Quanta 200 max instrument at 30 kV accelerating voltage. Thermogravimetry/differential thermal analysis (TG/DTA) measurements were performed using $\sim 15 \text{ mg}$ of the sample on a Dupont 9900/2100 system under nitrogen atmosphere (40 ml min^{-1}) with a heating rate of 10 K min^{-1} . Surface area analysis was performed on a Sorptomatic-1990 instrument. Before the measurement, the (calcined) sample was evacuated at 523 K for 12 h under vacuum (10^{-3} Torr). The surface area was calculated using the BET (Brunauer–Emmett–Teller) method and the pore size was estimated using the Horvath–Kawazoe technique. The pore volume was determined from the amount of nitrogen adsorbed at $P/P_0 = 0.5$.

Diffuse reflectance ultraviolet and visible (DRUV–VIS) spectra were recorded on UV-260 Shimadzu spectrophotometer with Whatman-40 filter paper as standard. The Fourier transform Raman (FT-Raman) spectra of the various samples (in powder form) was recorded on BRUKER RFS 100/S equipment. The excitation source used was a continuous wave Nd:YAG laser operates at 1064 nm with a liquid nitrogen cooled detector attached. The spectrum was collected after the Raleigh light was rejected by a super-notch filter. The number of scans and laser power used were 516 and 100 mW, respectively. Elemental analysis of the various samples was carried out using inductively coupled plasma–atomic emission spectroscopy (ICP–AES) technique on Labtam Plasma Lab 8440 equipment. The acidic behavior of the catalyst was studied by temperature programmed desorption of ammonia (TPDA). For

this purpose, ~ 400 mg of the catalyst was placed in quartz reactor and was activated at 823 K in air for 6 h followed by 2 h in helium with a flow rate of 50 ml min^{-1} . The reactor was then cooled to 373 K and maintained for another hour under the same condition. Ammonia adsorption was performed by passing the gas through the sample for ~ 15 –20 min at the same temperature. Subsequently, the system was purged with helium for an hour to remove the physisorbed ammonia, if any. Consequently, the desorption of ammonia was carried out by heating the reactor up to 873 K at a rate of 10 K min^{-1} using a temperature programmer (Eurotherm). The amount of ammonia desorbed was estimated with the aid of thermal conducting detector (TCD) response factor for ammonia.

2.4. Oxidation of cycloalkanes

The oxidation of cyclohexane (18 mmol) was carried out in presence of 5 mmol initiator (methyl ethyl ketone; MEK) at 373 K for 12 h under ambient pressure using 50 mg of the catalyst with 18 mmol of oxidant (30% H_2O_2) and 10 ml of solvent (acetic acid). After the reaction, the catalyst was separated and the products were extracted with ether and analyzed using gas chromatography (GC) with Carbowax column. The reaction was also performed using various other solvents such as methanol, tetrahydrofuran (THF) and acetone under the same reaction conditions. Furthermore, the influence of different initiators, e.g., cyclohexanone, acetaldehyde and acetone, as well as the effect of various oxidants, viz., air, oxygen (O_2) and TBHP, on the reaction was also investigated. On the other hand, the oxidation of cyclooctane (18 mmol) and cyclododecane (12 mmol) were executed under similar conditions as that of cyclohexane reaction except that mixed solvents (5 ml acetic acid + 5 ml dichloromethane) were used so as to make a homogeneous reaction mixture.

2.5. Recycling studies

After the first reaction run, the catalyst was filtered, washed with distilled water for three times and dried in an air-oven followed by activation at 773 K for 6 h. The activated catalyst was used for the subsequent recycling studies.

2.6. Washing studies

In order to remove non-framework titanium, if any, present in the matrix, the calcined catalyst (100 mg) was washed with 25 ml 1 M ammonium acetate for 12 h at room temperature under constant stirring. As before, the catalyst was filtered, repeatedly washed with water and then dried and activated at 773 K for 6 h. This catalyst is designated as washed catalyst.

2.7. Filtrate studies

In the filtrate study, the reaction was carried out with the filtrate collected at room temperature, i.e., the reaction mixture was cooled to RT and then filtered. The resulting filtrate solution was used to carry out the reaction.

2.8. Quenching studies

The reaction was also carried out with the filtrate (quenched solution) collected under reaction (hot) condition so as to establish the nature of the active species in the matrix.

3. Results and discussion

XRD patterns (Fig. 1) of all the as-synthesized Ti-HMA samples showed typical features characteristic of hexagonal MCM-41-type topology [13,15,30]. The four main reflections were resolved and indexed as 100, 110, 200 and 210. The average unit cell dimension (a_0) of all

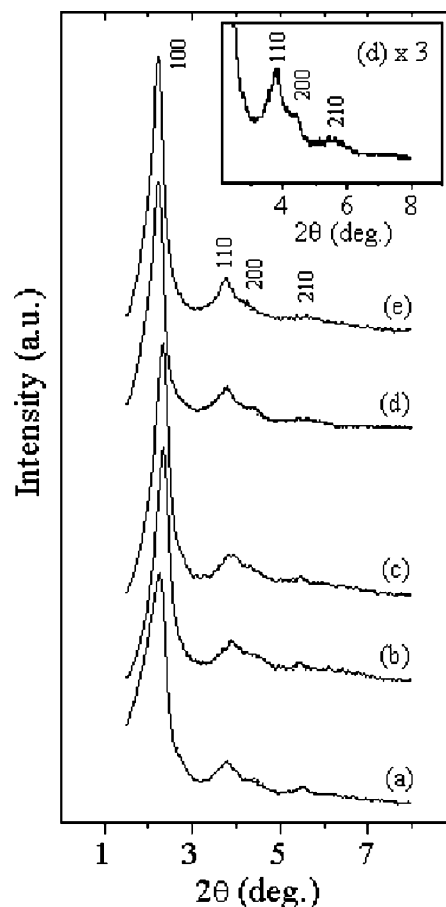


Fig. 1. XRD patterns of as-synthesized: (a) HMA, (b) TiHMA(200), (c) TiHMA(100), (d) TiHMA(50) and (e) TiHMA(25).

Table 1
XRD and ICP-AES data of TiHMA with different titanium content

Sample	[Al + P]/Ti (molar ratio)		Titanium content (wt.%)	Al/P	a_0 (Å) ^a	
	Synthesis gel	Calcined			As-synthesized	Calcined
HMA	–	–	–	1.36	45.4	33.7
TiHMA(200)	200	184	0.56	1.37	45.7	33.7
TiHMA(100)	100	80	1.27	1.39	46.5	37.1
TiHMA(50)	50	45	2.23	1.41	47.2	38.4
TiHMA(25)	25	21	3.25	1.42	47.6	38.8

^a a_0 is the average unit cell parameters of all the identified peaks.

the as-synthesized TiHMA samples (Table 1) were shifted to higher values compared to corresponding Ti-free HMA. The a_0 value increases with the increase in titanium content in the matrix indicating a possible substitution of titanium in the framework sites [31,32]. The increase in a_0 values may be due to the incorporation Ti^{4+} ions into the framework of HMA since Ti^{4+} has higher crystal radius (0.56 Å) as compared to either P^{5+} (0.31 Å) or Al^{3+} (0.52 Å) [33]. Fig. 2 depicts the XRD patterns of the corresponding calcined (TiHMA) samples. It is clear from this figure that, upon calcina-

tion, a decrease in unit cell dimension values was observed for all the samples due to the contraction of the framework as a consequence of the removal of the surfactant molecules. Furthermore, higher order reflections, viz., 110, 200 and 210, are disappeared and only a broad single reflection corresponding to 100 reflections is observed. This may be due to finite size effects of very fine particle morphology or due to the more disordered hexagonal framework structure of the samples [34–36]. This is ably supported by the TEM image and ED pattern of calcined TiHMA(50) where the samples show disordered hexagonal pattern [18]. It is also interesting to note that the mesoporous TiHMA(50) show that the crystallization of TiHMA samples take place in flower like agglomerates (Fig. 3a) while the analogous microporous TiAPO-5 crystallizes in tennis ball like shape (Fig. 3b).

ICP-AES analyses of the calcined HMA and TiHMA samples are summarized in Table 1. The increase in Al/P molar ratios with titanium content in the matrix indicates that Ti^{4+} replaces P^{5+} in TiHMA, which is in agreement with the XRD results. The decrease in molar ratios in calcined samples compared to the starting gel indicates the some of aluminium and/or phosphorous species were lost in the mother liquor during the synthesis. TG results of all the (TiHMA) samples showed a total weight loss of ~60–65% in three different stages corresponding to adsorbed water molecules, template and organic base [15]. On the other hand, the calcined TiHMA samples exhibit a weight loss of 20–23% due to the adsorbed water/gaseous molecules with corresponding endotherms at 383–393 K in DTA indicating mesoporous nature of the samples. Representative thermograms of both as-synthesized TiHMA(50) and calcined TiHMA(50) are presented in Figs. 4 and 5, respectively. In addition, nitrogen adsorption–desorption isotherm studies confirm the mesoporous nature of all the samples (Table 2). A representative nitrogen sorption plot showing type IV type isotherm, typical of mesoporous molecular sieves [37], of calcined TiHMA(50) is given in Fig. 6. As the relative pressure increases ($P/P_0 > 0.2$), the isotherm exhibits an inflection characteristic of capillary condensation within the mesopores. Adsorption at low relative pressures ($P/P_0 < 0.2$) is caused by monolayer adsorption of

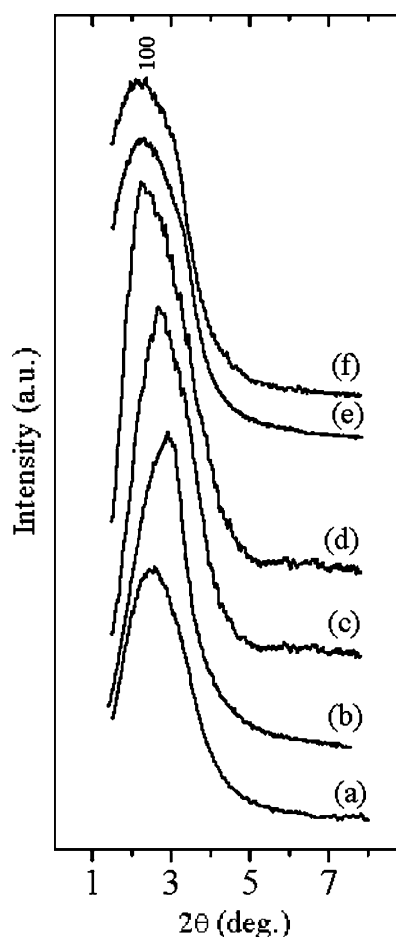


Fig. 2. XRD patterns of calcined: (a) HMA, (b) TiHMA(200), (c) TiHMA(100), (d) TiHMA(50), (e) TiHMA(25) and (f) TiHMA(50) after cyclohexane oxidation.

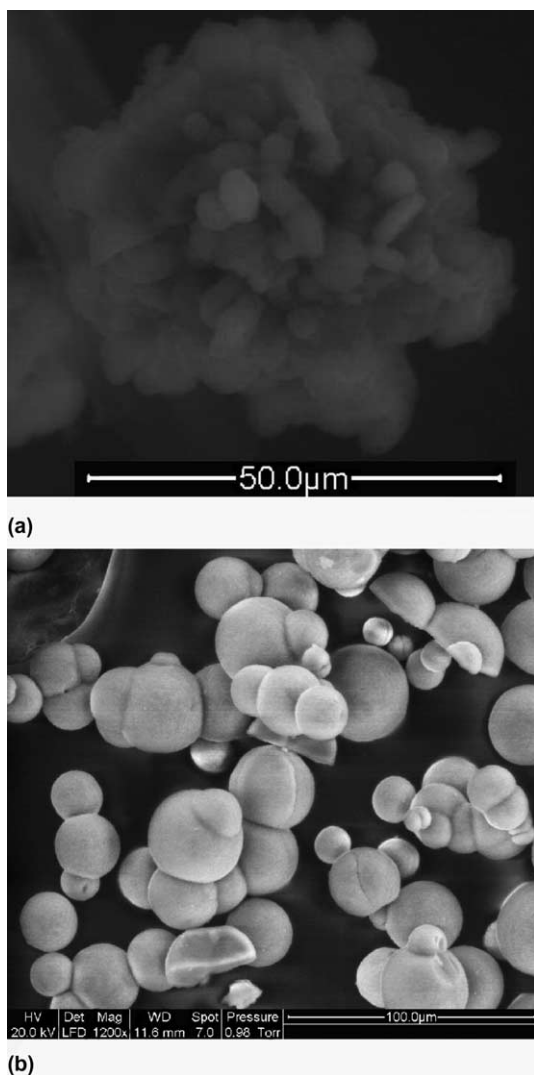


Fig. 3. E-SEM of: (a) calcined TiHMA(50) and (b) calcined TiAPO-5.

nitrogen on the walls of the mesopores. At $P/P_0 = 0.5$, the calculated pore volume was $0.52 \text{ cm}^3 \text{ g}^{-1}$ and the specific surface area was $953 \text{ m}^2 \text{ g}^{-1}$. Further, a narrow pore size distribution was noticed (see Fig. 6, inset) with a mesopore diameter of 29 \AA .

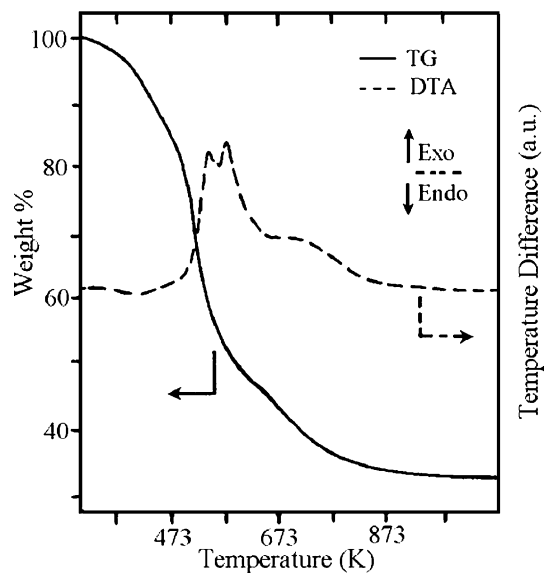


Fig. 4. TG-DTA of as-synthesized TiHMA(50).

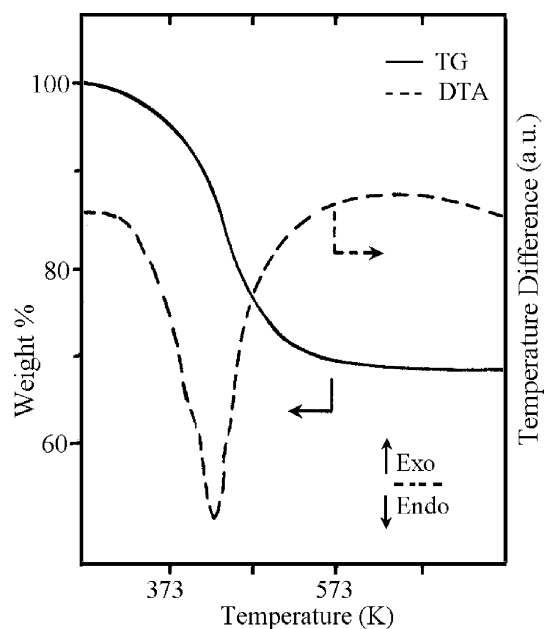


Fig. 5. TG-DTA of calcined TiHMA(50).

Table 2
Structural parameters of calcined TiHMA and TiMCM-41

Sample	S_{BET} ($\text{m}^2 \text{ g}^{-1}$)	Pore volume (ml g^{-1})	H-K pore diameter (\AA)	FWT (\AA) ^a
HMA	985	0.47	25	8.7
TiHMA(200)	960	0.54	25	9.2
TiHMA(100)	990	0.50	26	10.1
TiHMA(50)	953	0.52	29	9.4
TiHMA(50) ^b	925	0.50	29	9.3
TiHMA(25)	935	0.47	30	8.8
MCM-41	1080	0.80	30	10.5
TiMCM-41	1070	0.85	31	12.4

^a Framework wall thickness (FWT) = a_0 – H-K pore diameter.

^b After used for cyclohexane oxidation.

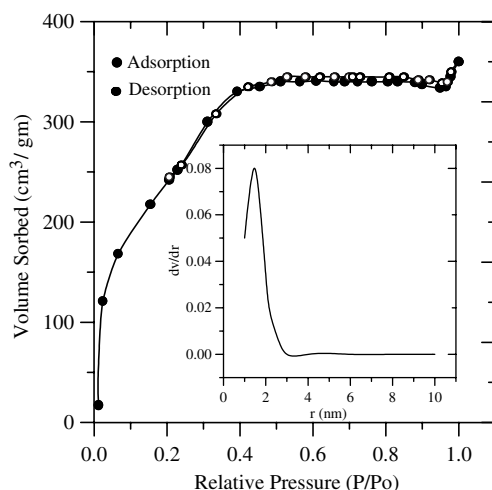


Fig. 6. Nitrogen adsorption-desorption isotherms of calcined TiHMA(50). The inset shows pore size distribution.

DRUV-VIS spectra (Fig. 7) of all the as-synthesized TiHMA samples showed a strong absorption band in the range 200–300 nm having peak maxima ~ 230 nm and a strong shoulder at 215 nm corresponding to charge transfer transitions [$O^{2-} \rightarrow Ti^{4+}$] of isolated tetrahedral Ti^{4+} species in the framework [32]. It is to be noted here that in the case of highly crystallized TS-1 [32] and Ti-BEA [38] samples the absorption maximum

was observed ~ 210 nm while in the case of semi-crystalline/amorphous TiMCM-41 [39] and TiHMS [40] samples the same was observed in the range 220–240 nm. On the other hand, this absorption maximum was noticed at 230–240 nm for titanium aluminophosphates [41,42]. Thus the position of peak maxima of the tetrahedral titanium species depends upon the coordinating atoms in the matrix, crystallinity, and the crystal size of the molecular sieves [43]. In addition to these, a shoulder ~ 270 nm was also observed which further increases upon increasing the titanium content in the samples. This could be attributed to reversible water coordinated pentavalent/hexavalent titanium species or due to the presence of small amount of titanium oxide clusters, which is generally observed in most of the high titanium loaded molecular sieves [39,40,44]. It is interesting to note that after calcination, no significant change was noted indicating the stability of the tetrahedral titanium species in the matrix (Fig. 8). For a comparison, the spectrum of TiO_2 is also shown (Fig. 8, curve e), which shows an absorption in the range of 300–500 nm with maxima at 330 nm. This feature is absent in all these TiHMA samples confirming the absence of any bulk TiO_2 impurity phase [32]. The absence of TiO_2 in both TiHMA(50) and TiHMA(25) samples was confirmed by

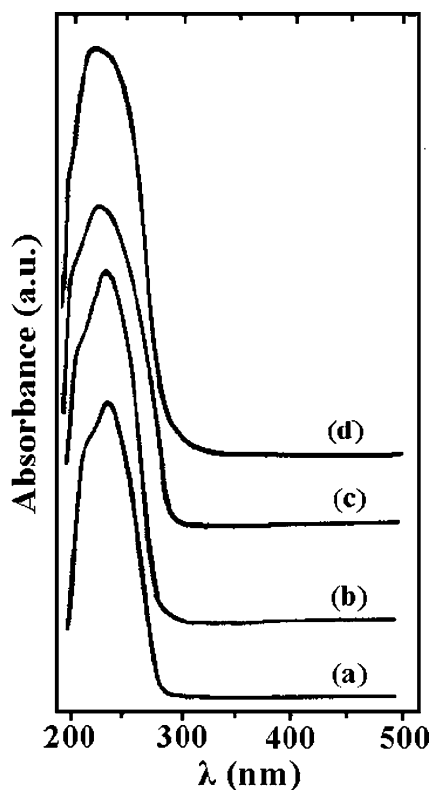


Fig. 7. DRUV-VIS spectra of as-synthesized: (a) TiHMA(200), (b) TiHMA(100), (c) TiHMA(50) and (d) TiHMA(25).

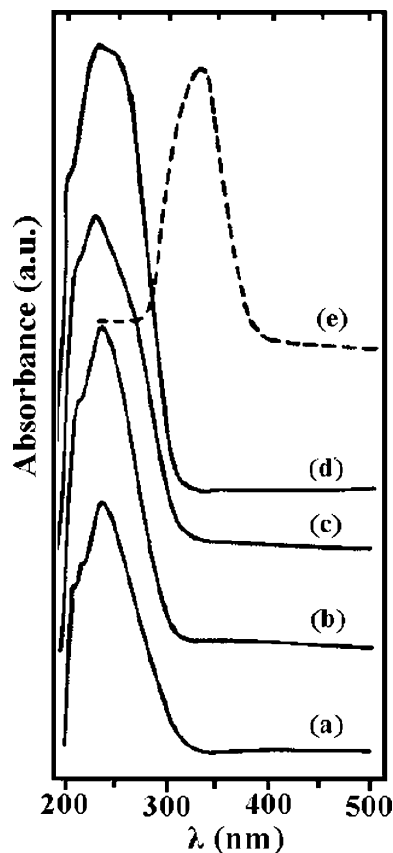


Fig. 8. DRUV-VIS spectra of calcined: (a) TiHMA(200), (b) TiHMA(100), (c) TiHMA(50), (d) TiHMA(25) and (e) TiO_2 .

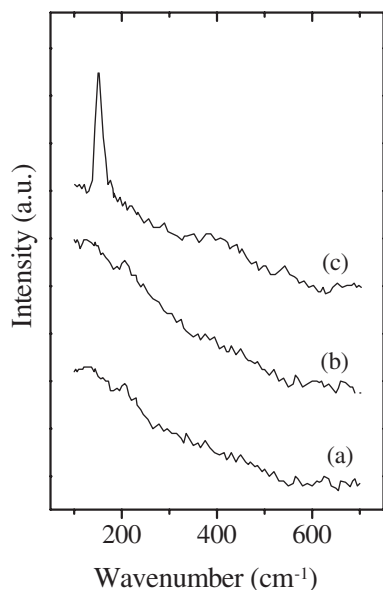


Fig. 9. FT-Raman spectra of: (a) calcined TiHMA(50), (b) calcined TiHMA(25) and (c) 1% TiO₂ mixed (calcined) TiHMA(50).

FT-Raman spectroscopy (Fig. 9a and b) wherein the absence of the absorption feature at $\sim 140\text{ cm}^{-1}$ is noticed [32] while it is clearly noticed in the case of 1% TiO₂ mixed TiHMA(50) sample (Fig. 9c).

Fig. 10a and b displays TPDA profiles of calcined HMA and TiHMA(50), respectively. The desorption pattern of titanium free HMA consists of two distinct peaks concentrated at 440 and 840 K. Deconvolution of

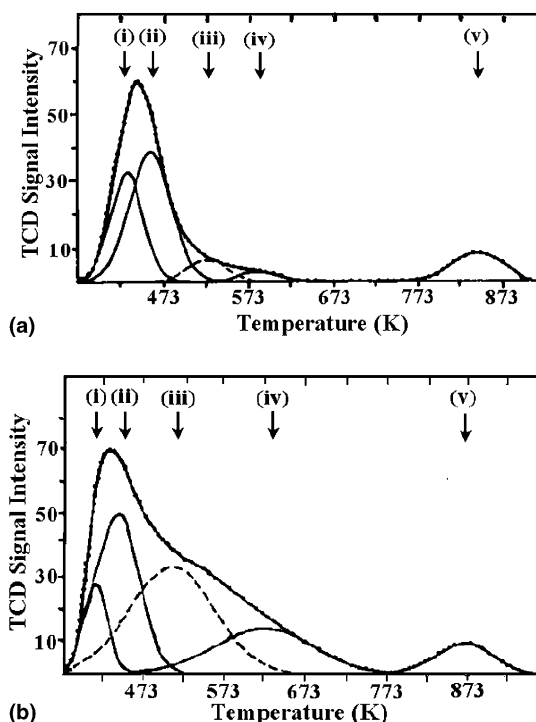


Fig. 10. TPDA of: (a) calcined HMA and (b) calcined TiHMA(50).

the TPDA profiles of both HMA and TiHMA(50) using Gaussian function with temperature as variant showed five peaks. The first two peaks (type-I and II) are attributed to the weak Brönsted acid sites. Type-III and IV peaks correspond to the structural acid sites whose percentages are increased significantly from HMA (10%) to TiHMA(50) (55%) indicating the incorporation of Ti⁴⁺ for P⁵⁺. The type-V curve is attributed to the Lewis acidic centers. The desorption peak at lower temperature range may consist of P–OH and/or Al–OH defect sites in the matrix corresponding to weak Brönsted acid sites. Similar weak Brönsted acid sites were also reported in literature [45–47]. The peak at higher temperature is corresponding to the Lewis acid characteristics of the sample. On the other hand, TiHMA showed a strong shoulder around 550–600 K, which may correspond to the structural Brönsted acid sites generated by the incorporation of Ti⁴⁺ for P⁵⁺. A similar observation was also reported for TiAPO_n molecular sieves [48]. It is likely that in the case of aluminophosphate molecular sieves, partial hydrolysis of Al–O–P bonds according to the reaction: $\text{Al–O–P} + \text{H}_2\text{O} \leftrightarrow \text{Al–OH} + \text{HO–P}$, results in weak Brönsted acid sites [49]. On the other hand, the peak at higher temperature range may arise possibly due to the presence of tricoordinated aluminium and/or octahedral aluminium oxide or oxyhydroxide species present in the matrix due to incomplete condensation of the network [45,46,50]. It is also demonstrated in literature that framework titanium can also act as a Lewis acid center in titanium containing molecular sieves [51].

Table 3 summarizes the oxidation results of cyclohexane over different amount of titanium containing HMA catalysts. It can be seen from this table that with the increase of titanium content in the catalyst, the substrate conversion increases, however, the selectivity towards cyclohexanol selectivity decreases. That is, TiHMA(200) and TiHMA(100) showed nearly 100% selectivity, however, with a lower conversion as compared to both TiHMA(50) and TiHMA(25). On the other hand, in the case of TiHMA(25), no significant improvement in the conversion was noticed but the selectivity towards cyclohexanol decreased and hence for all further studies was carried out over TiHMA(50) catalyst. Fig. 11 shows the effect of catalyst wt.% (w.r.t. cyclohexane) on the oxidation of cyclohexane. It can be seen from this figure that the conversion increases upto 3.3 wt.%, after which it almost saturates. Hence, for further studies, 3.3 wt.% of the catalyst was used. Fig. 12 depicts the effect of reaction time on the cyclohexane oxidation over TiHMA(50). It can be seen from this figure that cyclohexane conversion increases with time and saturates at 12 h. Further, increase of time does not affect the conversion significantly as 95% (iodometric titration) H₂O₂ was consumed during the 12 h period. On the other hand, after 12 h period of the reaction, the

Table 3

Effect of titanium concentration on the oxidation of cyclohexane^a

Catalyst	Conversion (wt.%)	Selectivity (wt.%)		
		Cyclohexanol	Cyclohexanone	Others
TiHMA(200)	54.2	100	–	–
TiHMA(100)	76.6	100	–	–
TiHMA(50)	86.2	98.4	1.2	0.4
TiHMA(25)	90.3	94.8	2.3	2.9

^a Reaction conditions: substrate: oxidant (H_2O_2) = 1:1; catalyst = 50 mg (3.3 wt.% of substrate); solvent (acetic acid) = 10 ml; MEK = 5 mmol; temperature = 373 K; time = 12 h.

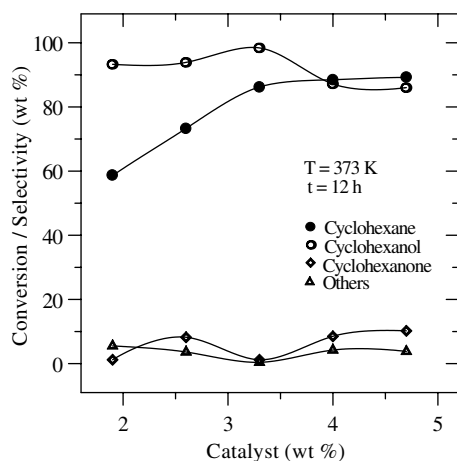


Fig. 11. Effect of catalyst concentration on the oxidation of cyclohexane over TiHMA(50).

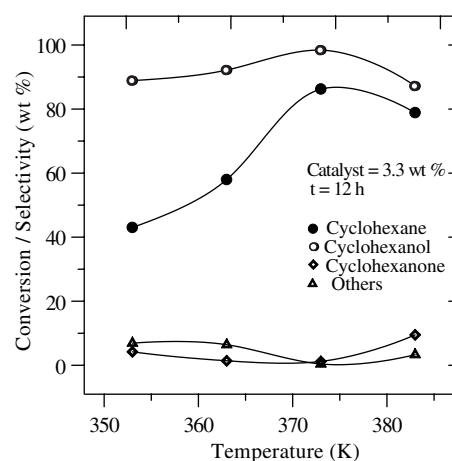


Fig. 13. Effect of reaction temperature on the oxidation of cyclohexane over TiHMA(50).

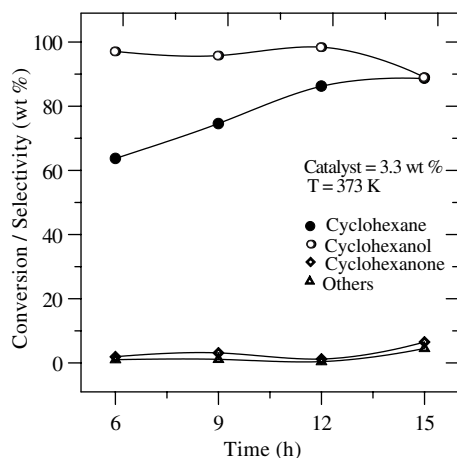


Fig. 12. Effect of reaction time on the oxidation of cyclohexane over TiHMA(50).

cyclohexanol selectivity decreases considerably owing to the secondary oxidation of cyclohexanol to cyclohexanone and cyclohexyl acetate. The reaction was also carried out in the temperature range 353–383 K, and the results are presented in Fig. 13. It can be seen from this figure that by increasing temperature, the activity increases up to 373 K where high conversion and excellent

cyclohexanol selectivity was observed. At higher temperature (>373 K), the possibility of H_2O_2 decomposition increases and therefore a decrease in the conversion. In addition, a significant amount of cyclohexanone was obtained due to the secondary oxidation.

From the above studies, it may be deduced that the optimized conditions for the oxidation of cyclohexane over TiHMA(50) catalyst with good conversion and selectivity are the following: catalyst amount = 3.3 wt.% (w.r.t. cyclohexane); time = 12 h, temperature = 373 K; oxidant (H_2O_2) to substrate (molar) ratio = 1, substrate/MEK (molar) ratio = 3.6; solvent = acetic acid. Under these specified conditions, a maximum cyclohexane conversion (86.2%) and cyclohexanol selectivity (98.4%) was obtained for TiHMA(50) with a trace amount of cyclohexanone and others products mostly cyclohexyl acetate (Table 4). As can be seen from this table that Ti-free HMA, blank (no catalyst) and TiO_2 showed only ~10% conversion under the identical experimental conditions. This clearly suggests that the high catalytic activity of TiHMA is mainly due to the presence of isolated tetrahedral Ti^{4+} ions as well as the mild reaction conditions. In order to check the stability of the Ti^{4+} ions in the TiHMA matrix, several recycling and washing experiments were performed, and it was found that the catalyst showed good recyclability without

Table 4
Oxidation of cyclohexane over various Ti-molecular sieves^a

Catalyst	Conversion (wt.%)	Titanium content ^b (wt.%)	Selectivity (wt.%)		
			Cyclohexanol	Cyclohexanone	Others
TiHMA(50)					
Calcined	86.2	2.23	98.4	1.2	0.4
Filtrate	9.8	—	95.2	2.3	2.5
Quenched solution	10.2	—	86.1	1.9	12.0
Recycled ^c	85.6	2.20	89.7	9.4	0.9
Washed	85.1	2.21	96.2	3.3	0.5
HMA	9.8	—	82.8	1.3	15.9
TiMCM-41					
Calcined	88.3	1.92	96.6	3.3	0.4
Filtrate	11.2	—	90.2	0.8	9.0
Quenched solution	10.8	—	89.0	1.2	9.8
Recycled ^c	86.0	1.89	88.7	9.4	1.9
Washed	88.7	1.88	92.7	6.3	1.0
MCM-41	11.6	—	96.4	—	3.6
Blank	9.0	—	78.1	—	21.9
TiO ₂	15.5	—	47.8	36.4	15.8

^a Reaction conditions: substrate: oxidant (H₂O₂) = 1:1; catalyst = 50 mg (3.3 wt.% of substrate); solvent (acetic acid) = 10 ml; MEK = 5 mmol; temperature = 373 K; time = 12 h.

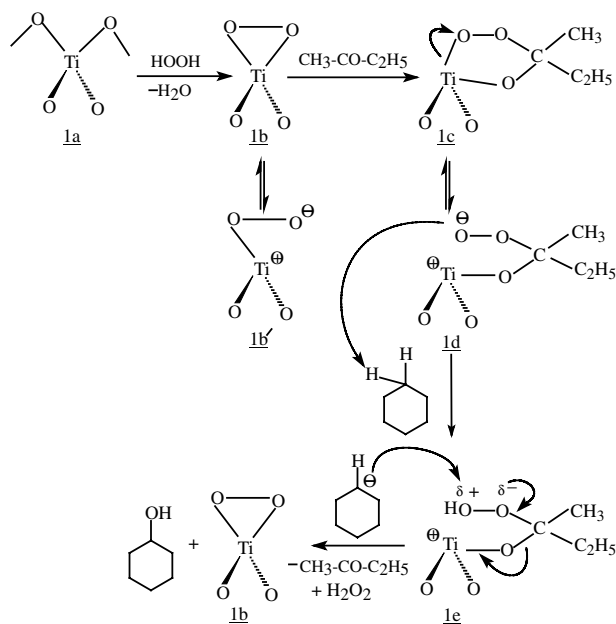
^b From ICP-AES analysis.

^c 3rd recycle or 4th run.

much loss inactivity. This is well supported by the XRD and nitrogen sorption isotherm measurements wherein the structure (see Fig. 2f) and porosity (see Table 2) remained unaltered even after various treatments. On the other hand, the non-leaching the active titanium species from the framework structure of TiHMA was further confirmed from the reaction carried over filtrate and quenching studies (see Table 4) as only a very low activity was observed in both the cases. Furthermore, this observation is well supported by ICP-AES analysis wherein no titanium was detected either in the filtrate solution or in the quenched solution. Thus, these studies confirm that the total conversion showed by TiHMA was due to the active Ti⁴⁺ species in the tetrahedral framework and hence it behaves truly as heterogeneous catalyst. In addition, TiHMA showed much higher activity than the analogous TiMCM-41. That is, after 6 h reaction period, TiHMA gave 65% conversion while TiMCM-41 showed only 42% conversion. This strongly suggests that the initial rate of reaction is faster in TiHMA than in TiMCM-41. This may be attributed to easy accessibility of active titanium sites in TiHMA than TiMCM-41 as due to a lower pore wall thickness (see Table 2) of the former than the latter, which allows more titanium sites to be exposed to the substrates and oxidants.

As far as the reactivity of the TiHMA is concerned, in general, it is known that the titanium species either titanil or tripodal titanium or tetrapodal titanium reacts with peroxide to give titanium peroxo species, which is generally the active species for the oxidation reaction with titanium and in presence of peroxides [52–54]. The formation of these species is confirmed, under the

reaction conditions, by the color change of the catalyst from white to yellow [55–59]. A similar peroxo-type species of Mo⁶⁺ and W⁶⁺ were also demonstrated earlier for the epoxidation reactions [60]. On this basis, we propose here a possible reaction pathway for the oxidation of cyclohexane over TiHMA (Scheme 1). As can be seen from this scheme that in absence of initiator, the reaction follows through the active species **1b'**, which abstracts hydrogen from cyclohexane [61] while in



Scheme 1. Reaction pathway of the oxidation of cyclohexane over TiHMA catalyst.

Table 5
Effect of different oxidants on the oxidation of cyclohexane over TiHMA(50)^a

Oxidant	Conversion (wt.%)	Selectivity (wt.%)		
		Cyclohexanol	Cyclohexanone	Others
H ₂ O ₂	86.2	98.4	1.2	0.4
TBHP	65.1	24.6	70.0	5.4
O ₂	47.2	92.3	5.6	2.3
Air	34.8	90.8	1.3	7.9

^a Reaction conditions: substrate: oxidant (H₂O₂ or TBHP) = 1:1; air and O₂ flow = 20 ml min⁻¹; catalyst = 50 mg (3.3 wt.% of substrate); solvent (acetic acid) = 10 ml; MEK = 5 mmol; temperature = 373 K; time = 12 h.

presence of an initiator (aldehyde or ketone), the reaction goes through active species **1c** and **1d**. Finally, hydroxyl transformation from (**1e**) to the resulting radical gives cyclohexanol. In this process, the initiator and the catalytic active site (**1b**) are regenerated. Since the electron density over the active oxygen on (**1b'**) is much lower than (**1d**), only 22% conversion was obtained without initiator whereas in presence of initiator it was 86%.

The reaction was also carried out over TiHMA employing different oxidants, viz., 70% TBHP, molecular O₂ and air. Table 5 summarizes the salient results along with the results obtained with H₂O₂. It is, however, clear from this table that the reaction with H₂O₂ exhibits much higher activity than that with the other oxidants. Furthermore, the increase of the amount of H₂O₂ results in nearly a complete oxidation with 99.2% cyclohexane conversion at 82% cyclohexanol and 14% cyclohexanone selectivity (Fig. 14). This observation is in good agreement with that noted for TS-2 catalyst [62]. On the other hand, TBHP gave cyclohexanone as the major product, owing to the much stronger oxidizing capability of TPHP than H₂O₂ [63], but with a lower conversion, which may be due the deactivation of the catalyst by the formation of *tert*-butanol upon decomposition of TBHP. When the reaction was carried out using molecular O₂ and air, a low substrate conversion but with good cyclohexanol selectivity. The low conversion may be due to a direct attack of O₂ on cyclohexane, an endothermic reaction, and as a consequence the activation process is highly difficult. Hence, various other oxidants, viz., idosobenzene [64,65], H₂O₂ [9,66–69] and alkylhydroperoxide [70–72] were in literature

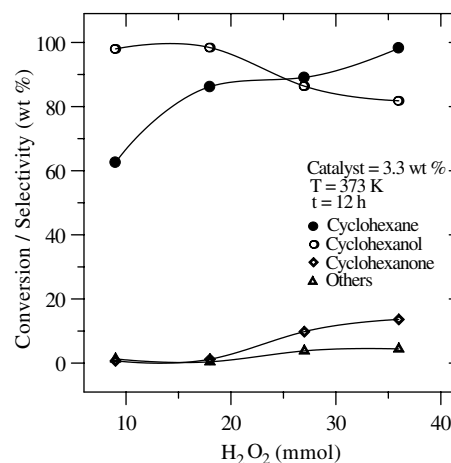


Fig. 14. Effect of H₂O₂ concentration on the oxidation of cyclohexane over TiHMA(50).

instead of energy consuming dioxygen activation. Amongst other oxidants, H₂O₂ is preferable because of simplicity in handling, environmentally friendly nature of coproduct (water), high oxygen atom efficiency and versatility [73–75].

Table 6 gives the influence of various solvents on the reaction over TiHMA. It can be seen from this table that a relatively lower conversion was obtained in the case of methanol, acetone, and tetrahydrofuran due to a possible partial decomposition of H₂O₂ under the reaction conditions. However, the observed higher catalytic activity in acetic acid can be attributed to the stabilization of H₂O₂ as peroxy acetic acid species. The influence of different initiator, e.g., MEK, acetone, cyclohexa-

Table 6
Effect of different solvents on the oxidation of cyclohexane over TiHMA(50)^a

Solvent	Conversion (wt.%)	Selectivity (wt.%)		
		Cyclohexanol	Cyclohexanone	Others
THF	18.0	70.0	30.0	0.0
Acetone	25.5	68.6	31.4	0.0
Methanol	28.4	74.6	17.0	8.4
Acetic acid	86.2	98.4	1.2	0.4

^a Reaction conditions: substrate: oxidant (H₂O₂) = 1:1; catalyst = 50 mg (3.3 wt.% of substrate); solvent = 10 ml; MEK = 5 mmol; temperature = 373 K; time = 12 h.

Table 7
Effect of different initiators on the oxidation of cyclohexane over TiHMA(50)^a

Initiator	Conversion (wt.%)	Selectivity (wt.%)		
		Cyclohexanol	Cyclohexanone	Others
MEK	86.2	98.4	1.2	0.4
Acetone	72.8	86.2	8.2	5.6
Cyclohexanone	58.5	83.5	9.3	7.2
Acetaldehyde	42.6	89.3	2.2	8.5

^a Reaction conditions: substrate: oxidant (H_2O_2) = 1:1; catalyst = 50 mg (3.3 wt.% of substrate); solvent (acetic acid) = 10 ml; initiator = 5 mmol; temperature = 373 K; time = 12 h.

none, and acetaldehyde, on the reaction was also studied and the results are listed in Table 7. It can be seen from this table that the use of acetaldehyde gives low activity due to the oxidation of acetaldehyde to acetic acid under the reaction conditions while the use of ketones results in good activity. MEK shows much better activity than acetone due to the electron releasing ability of ethyl group being more than methyl group. However, a further increase of MEK amount results in the secondary oxidation product cyclohexanone (Fig. 15). On the other hand, the lower activity of cyclohexanone is not clear, however, it may be due to the steric hindrance caused by the bulkier cyclohexane ring and/or symmetrical nature of cyclohexanone, which may hinder the formation of (1d) from (1c).

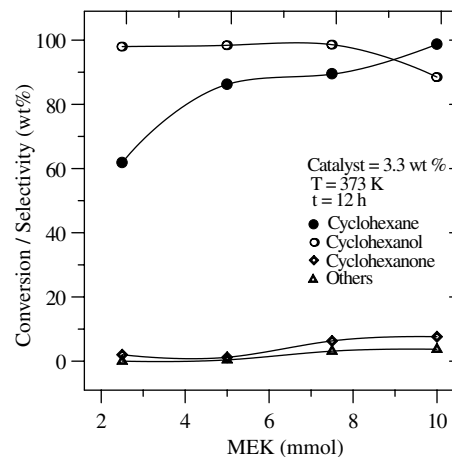


Fig. 15. Effect of MEK concentration on the oxidation of cyclohexane over TiHMA(50).

Table 8
Oxidation of cyclooctane over various Ti-molecular sieves^a

Catalysts	Conversion (wt.%)	Selectivity (wt.%)		
		Cyclohexanol	Cyclohexanone	Others
TiHMA(50)				
Calcined	85.0	81.5	15.2	3.3
Recycled ^b	83.5	78.0	18.0	1.5
TiMCM-41	82.0	80.5	10.0	9.5
TiAPO-5	23.5	68.5	17.0	11.8
TS-1	22.0	73.5	13.5	13.0

^a Reaction conditions: substrate: oxidant (H_2O_2) = 1:1; catalyst = 50 mg (2.48 wt.% of substrate); solvent = CH_3COOH (5 ml) + CH_2Cl_2 (5 ml); MEK = 5 mmol; temperature = 373 K; time = 12 h.

^b 3rd recycle or 4th run.

Table 9
Oxidation of cyclododecane over various Ti-molecular sieves^a

Catalysts	Conversion (wt.%)	Selectivity (wt.%)		
		Cyclohexanol	Cyclohexanone	Others
TiHMA(50)				
Calcined	87.0	75.5	20.0	4.5
Recycled ^b	85.5	68.8	25.0	6.2
TiMCM-41	81.0	64.8	27.0	8.2
TiAPO-5	26.0	66.2	18.1	15.7
TS-1	27.0	70.2	15.8	14.0

^a Reaction conditions: substrate: oxidant (H_2O_2) = 1:1; catalyst = 50 mg (2.48 wt.% of substrate); solvent = acetic acid (5 ml) + CH_2Cl_2 (5 ml); MEK = 5 mmol; temperature = 373 K; time = 12 h.

^b 3rd recycle or 4th run.

At this juncture, it is also interesting to note that both TiHMA and TiMCM-41 showed excellent activity for these bulkier cycloalkanes such as cyclooctane (Table 8) and cyclododecane (Table 9). Furthermore, TiHMA showed good recyclability for these substrates as well. On the other hand, the microporous analogues, viz., TiAPO-5 and TS-1, showed only meager activity towards these bulky substrates owing to their pore size restriction. Comparing the results of cyclohexane oxidation to these substrates, it was observed that more unidentified products were formed in bulkier substrates, resulting a decrease in selectivity of the required products, viz., alcohols (cyclooctanol and cyclododecanol) and ketones (cyclooctanone and cyclododecanone). The decrease in alcohol selectivity, however, could be due to the lower diffusion rate of the bulky cyclooctanol/cyclododecanol compared to cyclohexanol inside the mesopores.

4. Conclusion

TiHMA was hydrothermally synthesized with varying titanium content and characterized systematically using several analytical and spectroscopic techniques. A maximum of 3.25 wt.% of titanium could be incorporated in the tetrahedral framework mesoporous aluminophosphate matrix without forming any TiO₂ impurity phase. The catalyst exhibits excellent substrate conversion and product selectivity for the oxidation reactions of cycloalkenes, viz., cyclohexane, cyclooctane and cyclododecane, under mild reaction conditions as compared to many other catalysts reported so far. The presence of initiator (MEK) and solvent (acetic acid) was found to be essential and that the oxidant H₂O₂ was found to give highest catalytic activity. Further, cyclohexane reaction also gives good results when molecular oxygen and air used as oxidants. Finally, recycling studies as well as various other treatments such as washing, filtration and quenching clearly demonstrate that no leaching of the active species was observed under the reactions conditions thus suggesting TiHMA as a truly heterogeneous catalyst.

Acknowledgements

The authors thank RSIC/SAIF, IIT—Bombay for ICP-AES, TG-DTA, TEM, ED and SEM measurements. Thanks are also due to Dr. S. Sivasanker for a gift of TS-1 catalyst.

References

- [1] T. Katsuki, K.B. Sharpless, *J. Am. Chem. Soc.* 102 (1980) 5974.
- [2] R.A. Sheldon, *Stud. Surf. Sci. Catal.* 55 (1990) 1.
- [3] Shell Oil, British Pat. 1,249,079, 1971.
- [4] R.A. Sheldon, *J. Mol. Catal.* 7 (1980) 107.
- [5] M. Taramasso, B. Notari, US Pat. 4,410,501, 1983.
- [6] G. Bellusi, A. Carati, M.G. Clerici, A. Esposito, R. Millini, F. Buonomo, *Bel. Pat.* 1,001,038, 1989.
- [7] J.S. Reddy, R. Kumar, *Zeolites* 12 (1992) 95.
- [8] C. Perego, A. Carati, P. Ingallina, M.A. Mantegazza, G. Bellussi, *Appl. Catal. A* 221 (2001) 63.
- [9] T. Tatsumi, M. Nakamura, S. Negishi, H. Tominaga, *J. Chem. Soc. Chem. Commun.* (1990) 476.
- [10] M.A. Cambor, A. Corma, A. Martinez, J. Perez-Pariente, *J. Chem. Soc. Chem. Commun.* (1992) 589.
- [11] A. Tuel, *Zeolites* 15 (1995) 236.
- [12] N. Ulagappan, V. Krishnaswamy, *J. Chem. Soc. Chem. Commun.* (1995) 373.
- [13] C.T. Kresge, M.E. Leonowicz, W.J. Roth, J.C. Vertuli, J.S. Beck, *Nature* 359 (1992) 710.
- [14] D.T. On, D. Desplandier-Giscard, C. Danumah, S. Kaliaguine, *Appl. Catal. A* 222 (2001) 299.
- [15] T. Kimura, Y. Sugahara, K. Kuroda, *Chem. Lett.* (1997) 983; T. Kimura, Y. Sugahara, K. Kuroda, *Chem. Commun.* (1998) 559; T. Kimura, Y. Sugahara, K. Kuroda, *Micropor. Mesopor. Mater.* 22 (1998) 115; T. Kimura, Y. Sugahara, K. Kuroda, *Chem. Mater.* 11 (1999) 508.
- [16] M.P. Kapoor, A. Raj, *Appl. Catal. A* 203 (2000) 311.
- [17] X.S. Zhao, G.Q. Lu, *Micropor. Mesopor. Mater.* 44–45 (2001) 185.
- [18] S.K. Mohapatra, F. Hussain, P. Selvam, *Catal. Commun.* 4 (2003) 57.
- [19] E. Gianotti, E.C. Oliveira, S. Coluccia, H.O. Pastore, L. Marchese, *Inorg. Chem. Acta* 349 (2003) 259.
- [20] W.B. Fisher, J.F. Vanpappen, A.S. Inc, in: M. Howe-Grant, J.I. Kroschwitz (Eds.), *Kirk–Othmer Encyclopedia of Chemical Technology*, vol. 7, Wiley, New York, 1992, p. 851.
- [21] R.A. Sheldon, J.K. Kochi, *Metal Catalyzed Oxidation of Organic Compounds*, Academic Press, New York, 1981.
- [22] G.W. Parshall, S.D. Ittel, *Homogeneous Catalysis*, John Wiley, New York, 1992.
- [23] R.A. Sheldon, R.A. van Santen, *Catalytic Oxidation: Principles and Applications*, World Scientific, Singapore, 1995.
- [24] U. Schuchardt, D. Cardoso, R. Sercheli, R. Pereira, R.S. Cruz, M.C. Guerreiro, D. Mandelli, E.V. Spimace, E.L. Pires, *Appl. Catal. A* 211 (2001) 1, and references cited therein.
- [25] S.K. Mohapatra, B. Sahoo, W. Keune, P. Selvam, *Chem. Commun.* (2002) 1466.
- [26] A. Sakthivel, P. Selvam, *J. Catal.* 211 (2002) 134.
- [27] S.K. Mohapatra, F. Hussain, P. Selvam, *Catal. Lett.* 85 (2003) 217.
- [28] R.J. Mahalingam, P. Selvam, *Chem. Lett.* (1999) 455; R.J. Mahalingam, S.K. Badamali, P. Selvam, in: V. Murugesan, B. Arabindoo, M. Palanichamy (Eds.), *Recent Trends in Catalysis*, Narosa, New Delhi, 1999, p. 214.
- [29] A. Thangaraj, S. Sivasanker, *J. Chem. Soc. Chem. Commun.* (1992) 123.
- [30] P. Selvam, S.K. Bhatia, C.G. Sonwane, *Ind. Eng. Chem. Res.* 40 (2001) 3237.
- [31] T. Blasco, A. Corma, M.T. Navarro, J.P. Pariente, *J. Catal.* 156 (1995) 65.
- [32] G.N. Vayssilov, *Catal. Rev.—Sci. Eng.* 39 (1997) 209.
- [33] R.D. Shannon, *Acta Crystallogr. A* 32 (1976) 751.
- [34] P.T. Tanev, T.J. Pinnavaia, *Science* 267 (1995) 865.
- [35] S.A. Bagshaw, E. Prouzet, T.J. Pinnavaia, *Science* 269 (1995) 1242.
- [36] R. Ryoo, J.M. Kim, C.H. Ko, *J. Phys. Chem.* 100 (1996) 17718.
- [37] S. Storck, H. Bretinger, W.F. Maier, *Appl. Catal. A* 174 (1998) 137.

- [38] T. Blasco, M.A. Camblor, A. Corma, J.P. Pariente, *J. Am. Chem. Soc.* 115 (1993) 11813.
- [39] L. Marchese, E. Gianotti, T. Maschmeyer, G. Martra, S. Coluccia, J.M. Thomas, *Nuovo Cimento* 19 (1997) 1707.
- [40] S. Gontier, A. Tuel, *Zeolites* 15 (1995) 601.
- [41] A. Tuel, Y.B. Taarit, *J. Chem. Soc. Chem. Commun.* (1994) 1667.
- [42] M.H. Zahedi-Niaki, M.P. Kapoor, S. Kaliaguine, *J. Catal.* 177 (1998) 231.
- [43] A. Tuel, Y.B. Taarit, *Micropor. Mater.* 1 (1993) 179.
- [44] F. Geobaldo, S. Bordiga, A. Zecchina, E. Giamello, G. Leofanti, G. Petrini, *Catal. Lett.* 16 (1992) 109.
- [45] D. Arias, I. Campos, D. Escalante, J. Goldwasser, C.M. Lopez, F.J. Machado, B. Mendez, D. Moronta, M. Pinto, V. Sazo, M.M.R. de Agudelo, *J. Mol. Catal. A* 122 (1997) 175.
- [46] E. Dumitriu, V. Hulea, I. Fechete, A. Auroux, J.-F. Lacaze, C. Guimon, *Micropor. Mesopor. Mater.* 43 (2001) 341.
- [47] J. Das, C.V.V. Satyanaryana, D.K. Chakrabarty, S.N. Piramanayagam, S.N. Shringi, *J. Chem. Soc. Faraday Trans.* 88 (1992) 3255.
- [48] M.H. Zahedi-Niaki, S.M.J. Zaidi, S. Kaliaguine, *Micropor. Mesopor. Mater.* 32 (1999) 251.
- [49] B. Parltitz, U. Lohse, E. Schreier, *Micropor. Mater.* 2 (1994) 223.
- [50] H. Kosslick, G. Lischke, H. Landmesser, B. Parltitz, W. Storek, R. Fricke, *J. Catal.* 176 (1998) 102.
- [51] J.C. van der Wall, K. Tan, H. van Bekkum, *Catal. Lett.* 41 (1996) 63;
J.C. van der Wall, P.J. Kunkeler, K. Tan, H. van Bekkum, *J. Catal.* 173 (1998) 74.
- [52] P. Kumar, R. Kumar, B. Pandey, *Synth. Lett.* (1994) 289.
- [53] A. Bhaumik, P. Kumar, R. Kumar, *Catal. Lett.* 40 (1996) 47.
- [54] W. Adam, A. Corma, I. Reddy, M. Renz, *J. Org. Chem.* 62 (1997) 3631.
- [55] G. Schönn, *Z. Anal. Chem.* 9 (1870) 41.
- [56] J. Mühlebach, K. Müller, G. Schwarzenbach, *Inorg. Chem.* 9 (1970) 2381.
- [57] D. Schwarzenbach, *Inorg. Chem.* 9 (1970) 2381.
- [58] B. Notari, *Stud. Surf. Sci. Catal.* 37 (1988) 413.
- [59] D.R.C. Huybrechts, L. De Bruycker, P.A. Jacobs, *Nature* 345 (1990) 240.
- [60] G. Amato, A. Arcoria, F.T. Ballistreri, G.A. Tomaselli, O. Bortolini, V. Conte, F. Di Furia, G. Modena, G. Valle, *J. Mol. Catal.* 37 (1986) 165.
- [61] D.R.C. Huybrechts, P.L. Buskens, P.A. Jacobs, *J. Mol. Catal.* 71 (1992) 129.
- [62] J.S. Reddy, S. Sivasanker, *Catal. Lett.* 11 (1991) 241.
- [63] E.L. Pires, J.C. Magalhaes, U. Schuchardt, *Appl. Catal. A* 203 (2000) 231.
- [64] J.T. Groves, T.E. Nemo, *J. Am. Chem. Soc.* 105 (1983) 6243.
- [65] T.G. Traylor, J.S. Buyn, P.S. Trylor, P. Battoni, D. Mansuy, *J. Am. Chem. Soc.* 113 (1991) 7821.
- [66] J. Xiao, J. Xu, Z. Gao, *Catal. Lett.* 57 (1999) 37.
- [67] C. Sheu, S.A. Richert, P. Cofre, B.J. Ross, A. Sobkowiak, D.T. Sawyer, J.R. Kanotsky, *J. Am. Chem. Soc.* 112 (1990) 1936.
- [68] A.S. Goldstein, R.H. Beer, R.S. Drago, *J. Am. Chem. Soc.* 116 (1994) 2424.
- [69] N. Mizuno, C. Nozaki, I. Kiyoto, M. Misono, *J. Am. Chem. Soc.* 120 (1998) 9267.
- [70] R.F. Parton, G.J. Peere, P.E. Neys, P.A. Jacobs, R. Claessens, G.V. Baron, *J. Mol. Catal. A* 113 (1996) 445.
- [71] T. Maschmeyer, R.D. Oldroyd, G. Sankar, J.M. Thomas, I.J. Shannon, J.A. Klepetko, A.F. Masters, J.K. Beattie, C.R. Catlow, *Angew. Chem. Int. Ed. Engl.* 36 (1997) 1639.
- [72] P.A. Mac, I.W. Faul, C.E. Arends, K.U. Ingold, D.D.M. Wayner, *J. Chem. Soc., Perkin Trans.* 2 (1997) 135.
- [73] R.A. Sheldon, *Top. Curr. Chem.* 164 (1993) 23.
- [74] P. Knops-Gerrits, D.D. Vos, F. Thibault-Starzyk, P.A. Jacobs, *Nature* 369 (1994) 543.
- [75] C.L. Hill, C.M. Prosser-McCartha, *Coord. Chem. Rev.* 143 (1995) 407.